Lipid Lateral Heterogeneity in Phosphatidylcholine/Phosphatidylserine/ Diacylglycerol Vesicles and Its Influence on Protein Kinase C Activation

Andrew R. G. Dibble, Anne K. Hinderliter, Julianne J. Sando, and Rodney L. Biltonen
Department of Pharmacology, University of Virginia Health Sciences Center, Charlottesville, Virginia 22908 USA

ABSTRACT To test the hypothesis that the activation of protein kinase C (PKC) is influenced by lateral heterogeneities of the components of the lipid bilayer, the thermotropic phase behavior of dimyristoylphosphatidylcholine (DMPC)/dimyristoylphosphatidylserine (DMPS)/dioleoylglycerol (DO) vesicles was compared with the activation of PKC by this system. Differential scanning calorimetry (DSC) and Fourier transform infrared (FTIR) spectroscopy were used to monitor the main transition (i.e., the gel-to-fluid phase transition) as a function of mole fraction DO (χ_{DO}) in DMPC/DO, DMPS/DO, and [DMPC/DMPS (1:1, mol/mol)]/DO multilamellar vesicles (MLVs). In each case, when $\chi_{DO} < \sim 0.3$, DO significantly broadened the main transition and shifted it to lower temperatures; but when $\chi_{DO} > \sim 0.3$, the main transition became highly cooperative, i.e., narrow, again. The coexistence of overlapping narrow and broad transitions was clearly evident in DSC thermograms from $\chi_{DO} \approx 0.1$ to $\chi_{DO} \approx 0.3$, with the more cooperative transition growing at the expense of the broader one as χ_{DO} increased. FTIR spectroscopy, using analogs of DMPC and DMPS with perdeuterated acyl chains, showed that the melting profiles of all three lipid components in [DMPC/DMPS (1:1, mol/mol)]/DO MLVs virtually overlay when $\chi_{DO} = 0.33$, suggesting that a new type of phase, with a phospholipid/DO mole ratio near 2:1, is formed in this system. Collectively, the results are consistent with the coexistence of DO-poor and DO-rich domains throughout the compositions $\chi_{DO} \approx 0.1$ to $\chi_{DO} \approx 0.3$, even at temperatures above the main transition. Comparison of the phase behavior of the binary mixtures with that of the ternary mixtures suggests that DMPS/DO interactions may be more favorable than DMPC/DO interactions in the ternary system, especially in the gel state. PKC activity was measured using [DMPC/DMPS (1:1, mol/mol)]/DO MLVs as the lipid activator. At 35°C (a temperature above the main transition of the lipids), PKC activity increased gradually with increasing χ_{DO} from $\chi_{DO} \approx 0.1$ to $\chi_{DO} \approx 0.4$, and activity remained high at higher DO contents. In contrast, at 2°C (a temperature below the main transition), PKC activity exhibited a maximum between $\chi_{DO} \approx 0.1$ and $\chi_{DO} \approx 0.3$, and at higher DO contents activity was essentially constant at 20–25% of the activity at the maximum. We infer from these results that the formation of DO-rich domains is related to PKC activation, and when the lipid is in the gel state, the *coexistence* of DO-poor and DO-rich phases also contributes to PKC activation.

INTRODUCTION

Most biological membranes are composed of complex mixtures of lipids and proteins. Evidence for significant lateral heterogeneity of lipid and protein components in many types of model and cell membranes has been provided by a wide variety of experimental techniques (Edidin, 1992; Tocanne, 1992). The potential relevance of these heterogeneities to the functioning of biological membranes has recently been discussed (Bergelson et al., 1995). Of particular interest to us is the influence of lipid lateral heterogeneity on the activation of water-soluble enzymes at the membrane surface (i.e., interfacial activation). One important and relatively well-characterized enzyme that can bind to membrane surfaces and be activated there is protein kinase C (PKC). The activation of PKC is quite sensitive to membrane physical properties (reviewed in Sando et al., 1992), including the lateral distribution of lipids (Bazzi and Nelsestuen, 1987; Yang and Glaser, 1995). However, the detailed nature of the physical properties that contribute most significantly to PKC activation has remained elusive.

PKC is a family of at least 11 phospholipid-dependent serine/threonine-specific protein kinases (Stabel and Parker, 1991; Nakamura and Nishizuka, 1994), the members of which play central roles in a variety of physiological processes, including cell growth and differentiation (Nishizuka, 1986; Kikkawa et al., 1989). PKC isozymes are pivotal in the process of transmembrane signal transduction because enzymatic activation on the inner leaflet of the plasma membrane links extracellular signals to intracellular cascade reactions. Most cells express several PKC isozymes that differ in activation requirements, suggesting that different isozymes are involved in distinct signaling pathways. In in vitro vesicle systems, the activation of all PKC isozymes requires the acidic phospholipid phosphatidylserine (PS); activation also requires diacylglycerol (DAG) or phorbol ester tumor promotors for all isozymes except PKC-ζ and λ; PKC-α, β_I, β_{II}, and γ activity is also dependent on Ca^{2+} (Nakamura and Nishizuka, 1994).

DAG is produced in vivo by hormone- or growth factor-stimulated hydrolysis of phospholipid, especially phosphatidylinositol and phosphatidylcholine (PC), within the inner leaflet of the plasma membrane. PC-derived DAG tends to be degraded relatively slowly and is implicated in cellular control mechanisms associated with long-term PKC activa-

Received for publication 23 May 1996 and in final form 18 July 1996.

Address reprint requests to Dr. Rodney L. Biltonen, Departments of Biochemistry and Pharmacology, University of Virginia Health Sciences Center, Box 448, Charlottesville, VA 22908. Tel.: 804-924-2422; Fax: 804-982-0569; E-mail: rlb1t@virginia.edu.

0006-3495/96/10/1877/14 $2.00

tion (Exton, 1990; Nakamura and Nishizuka, 1994). DAG levels of only a few mole percent are sufficient to activate PKC in vivo (Preiss et al., 1986). However, some transformed cells have up to 10 mol% DAG because of the action of oncoproteins such as *ras*, *src*, and *erbB2* (reviewed in Basu, 1993).

In addition to DAG and PS, a wide variety of lipid-soluble molecules can modulate PKC activity. These include phorbol esters, lyso-phospholipids, fatty acids, phosphatidic acids, phosphatidylethanolamines, and long-chain alcohols (reviewed in Sando et al., 1992). Because PKC activity is sensitive to so many kinds of membrane components, physical properties of the membrane have been included in many models describing PKC membrane binding and activation. These properties include 1) a negative membrane surface potential due to the presence of acidic phospholipids, especially PS (Takai et al., 1979; Bazzi and Nelsestuen, 1987; Kim et al., 1991; Mosior and McLaughlin, 1991; Orr and Newton, 1992b); 2) increased spacing between phospholipid headgroups caused by the interposition of the relatively small headgroup of DAG (Das and Rand, 1986; Walker and Sando, 1988; Walker et al., 1990; Bolen and Sando, 1992; De Boeck and Zidovetzki, 1992; Slater et al., 1994); 3) regions of high bilayer curvature induced by lipids with relatively small polar headgroups in proportion to their ability to increase the hydrocarbon volume of the bilayer, e.g., phosphatidylethanolamine (Senisterra and Epand, 1993) and DAG (Dawson et al., 1984; Das and Rand, 1986; Epand and Bottega, 1988; Goldberg et al., 1994); and 4) decreased hydration of the membrane surface caused by, e.g., alcohol and DAG, presumably due to the formation of intermolecular hydrogen bonds between these molecules and neighboring phospholipids (Chiou et al., 1992; Heimburg et al., 1992; López-García et al., 1993, 1994b; Goldberg et al., 1995).

In addition to these membrane physical properties, there is good evidence that the activation of PKC requires specific lipid-protein interactions. For example, whereas PKC binding to membranes is facilitated by any acidic phospholipid, the L stereoisomer of PS is required for maximum PKC activation (Lee and Bell, 1989; Newton and Keranen, 1994). Similarly, 1,2-*sn*-DAG activates PKC, whereas the 1,3 and 2,3 isomers do not (Rando and Young, 1984; Rando, 1988). These observations suggest that PKC has binding sites for PS and DAG. Indeed, DAG has been shown to compete for phorbol ester binding to the C1 domain of PKC (Sharkey et al., 1984). The crystal structure of the cys2 domain (a portion of the C1 domain that includes the phorbol ester binding site) of PKC-δ has been determined both alone and in a complex with phorbol 13-acetate (Zhang et al., 1995). This study shows that phorbol ester binding does not produce a significant conformational change in the cys2 domain; rather, the binding alters the nature of the protein surface and in this way may stabilize a membrane-inserted state. Water-insoluble long-chain phorbol esters bind to PKC more strongly and activate PKC more potently, both by several orders of magnitude, than does DAG. It is likely that PKC activation by DAG and PS requires synergism between specific lipid-protein interactions and membrane physical properties. For instance, modulation of the surface charge density, the spacing between phospholipid headgroups, the exposure of regions of high bilayer curvature, and/or the hydration state of the membrane surface may allow PKC and its ligands to interact in a manner favorable for enzyme activation.

Although it is clear that physical properties of the membrane play an important role in PKC activation, the details of the mechanism of activation are still poorly understood. An important question is, how can the production of only a few mole percent of DAG in vivo change the physical properties of the cell membrane sufficiently to activate PKC? One possibility is that DAG is not randomly distributed but is found in clusters with a relatively high local DAG concentration. Such DAG-rich domains could form by the rapid and localized hydrolysis of phosphatidylinositol or PC. (We use the term "domain" to refer to regions of the membrane that have a local lipid composition distinct from the composition of the overall vesicle. We distinguish between types of domains by noting which lipid components are depleted or enriched in these regions.) There is also evidence that DAG has a tendency to demix at equilibrium in PC/DAG binary mixtures (Ortiz et al., 1988; Cunningham et al., 1989; Heimburg et al., 1992; López-García et al., 1994b; Quinn et al., 1995). PC and DAG have very different hydration states and propensities to induce negative curvature in bilayers, and it is probable that both of these properties contribute to the observed demixing.

In the present work, we test the specific hypothesis that PKC is activated by the formation of DAG-rich domains in membranes. We use PC/PS/DAG vesicles because they are stable and characterizable bilayers that can activate PKC (Boni and Rando, 1985). Previous work with PC/PS/dioleoylglycerol (DO) (70:25:5, mol/mol) vesicles revealed a correspondence between the number of *cis*-monounsaturated acyl chains in the system and PKC activation (Bolen and Sando, 1992). However, as the mole fraction of DO (χ_{DO}) is increased from 0.05 to 0.25, the saturated system of dimyristoyl-PC (DMPC)/dimyristoyl-PS (DMPS)/DO gradually becomes as effective at activating PKC as a system with fully monounsaturated phospholipids (i.e., dioleoyl-PC/dioleoyl-PS/DO). In the present study, we focus on the DMPC/DMPS/DO system because its ability to activate PKC varies greatly over a wide range of compositions and its main transition (i.e., gel-to-fluid phase transition) is near room temperature, allowing a description of the phase behavior of the system as well as a comparison of the ability of gel-state and fluid-state lipid to activate PKC. We present evidence that DO-poor and DO-rich domains coexist over a wide range of compositions (from $\chi_{DO} \approx 0.1$ to $\chi_{DO} \approx 0.3$) in DMPC/DMPS/DO mixtures, even at temperatures above the main transition, and that the formation of the DO-rich domains is important for PKC activation.

MATERIALS AND METHODS

Materials

All lipids were from Avanti Polar Lipids (Birmingham, AL) and were judged to be >99% pure by thin-layer chromatography of 0.1 mg of each lipid on Adsorbosil-Plus 1 P plates (Alltech Associates, Deerfield, IL), using the solvent systems chloroform/methanol/acetic acid/water (50:30:8:4, v/v) for PS; chloroform/methanol/water (65:25:4, v/v) for PC, and petroleum ether/ethyl ether/acetic acid (160:40:2, v/v) for DO to determine purity, and chloroform/acetone (95:5, v/v) to determine the extent of isomerization (i.e., acyl chain migration yielding 1,3-dioleoyl-*sn*-glycerol). Lipid purity and extent of DO isomerization were checked with several samples before and after the differential scanning calorimetry (DSC) experiments and PKC assays. Lipid breakdown did not exceed 1%. We estimated the extent of isomerization of DO in chloroform stock solutions to be <1%, and of DO in temperature-cycled vesicles to be <10%.

The calcium ionophore antibiotic A23187 was from Calbiochem Corp. (La Jolla, CA). The stock solution of [γ-^{32}P]ATP (7000 Ci/mmol) was from ICN Pharmaceuticals (Costa Mesa, CA). Histone (type III-S) and phorbol esters were from Sigma Chemical Co. (St. Louis, MO). Grace's culture medium, yeastolate, lactalbumin, and fetal calf serum for the culturing of Sf-9 insect cells were from GIBCO (Grand Island, NY). 3-Morpholinopropanesulfonic acid (MOPS) (BioChemika grade), EGTA (Chemika grade), potassium chloride (Chemika grade), and magnesium chloride hydrate (puriss grade) were from Fluka Chemical Corp. (Ronkonkoma, NY). Chloroform, methanol, and benzene were high-performance liquid chromatography grade (Fisher Scientific, Pittsburgh, PA) or Baker Analyzed (J.B. Baker, Inc., Bricktown, NJ). All other chemicals were reagent grade.

Preparation of solutions

Water was double distilled through glass. Before weighing, the potassium chloride was dried to a constant weight with gentle heating and the magnesium chloride hydrate was dried to a stoichiometric hydrate, $MgCl_2 \cdot 4H_20$, by heating at 100°C for 1 h. The primary standard phosphate solution in water was prepared from an analytical concentrate (J.T. Baker, Inc.). The concentration of phospholipid stock solutions in chloroform was periodically determined by phosphorus analysis (Kingsley and Feigenson, 1979). All lipid stock solutions were stored under an argon atmosphere, at ≤ -20°C.

Preparation of multilamellar vesicles

Mixtures of DO and phospholipid were prepared by aliquoting stock solutions of lipid in chloroform into borosilicate culture tubes using gas-tight syringes (Hamilton Co., Reno, NV). To all samples for DSC and PKC activity assays, the ionophore A23187 in chloroform was added at a ionophore/total phospholipid mole ratio of 1:1000. (The ionophore was included to facilitate the equilibration of Mg^{2+} across hydrated bilayers; see below.) Samples were dried to a thin film under a stream of nitrogen and then were either put directly on a vacuum line or lyophilized from benzene/methanol (19:1, v/v) for a minimum of 12 h in the dark. The two methods of lipid-drying yielded essentially identical results. Each dried sample was hydrated under argon with 20 mM MOPS, 100 mM KCl, 0.1 mM EGTA, pH 7.5 (i.e., MOPS/KCl buffer). Each sample was temperature cycled through the main transition at a rate not exceeding 0.5°C/min at least two times before briefly vortexing at a temperature above the main transition. Samples not appearing homogeneous at this stage (e.g., DMPC/DO when $\chi_{DO} > \sim 0.3$) were temperature cycled and vortexed further. Multilamellar vesicles (MLVs) treated with Mg^{2+} were diluted 4:1 (v/v) with MOPS/KCl buffer containing 25 mM $MgCl_2$, and slowly temperature cycled at least two more times. All MLVs were stored in the dark under an argon atmosphere at room temperature.

Differential scanning calorimetry

Excess heat capacity functions of MLVs (1.4 ml of 9.3–10 mM total phospholipid) were obtained at +10°C/h using a MicroCal MC-2 scanning calorimeter. No baselines were subtracted, and the data were not corrected for the time response of the instrument (the time constant is <10 s). From the heating scans, onset and termination temperatures (i.e., apparent solidus and liquidus temperatures) of the main transition were estimated as follows. First, the two temperatures at which a thermogram deviates from baseline were estimated by eye. Next, the apparent enthalpy change, as estimated by integrating the curve between these two temperatures, was measured. Finally, the end points of this integration were simultaneously shifted toward one another until the area of the curve was reduced to 96% of the total apparent enthalpy change. This method reduced the variation in estimating the onset and termination of extremely broad thermograms.

Fourier transform infrared spectroscopy

MLVs at 15 mM total phospholipid were prepared as described. After a minimum of 1 day of hydration, MLVs were pelleted with a clinical centrifuge. This concentrated sample (50–100 mM lipid) was injected between CaF_2 windows separated by a 25-μm Teflon spacer of a thermostated transmission cell (Harrick Scientific, Ossining, NY), modified as described by Doebler and Holloway (1993). The temperature of the cell was controlled with a circulating temperature bath (Neslab Instruments, Newington, NH), with a remote temperature probe housed against the edge of the cell window. The bath was interfaced to the spectrometer computer that regulated the temperature set point. The set point was changed by 0.5–2.0°C between isothermal spectra. After reaching a new set point, the sample was allowed to equilibrate for 3 min before data collection was resumed. Temperature was stable within $\pm$ 0.02°C. Interferograms were collected using a Nicolet 740 Fourier transform infrared (FTIR) spectrometer equipped with a mercury cadmium telluride detector cooled with liquid nitrogen. To remove atmospheric water vapor, the spectrometer was purged continuously with dry air. Each spectrum consists of 1000 interferograms co-added and apodized with a Happ-Genzel apodization function and Fourier transformed to yield a spectral resolution of 2 cm^{-1}. The center of mass of CH_2 antisymmetric (~2920 cm^{-1}), CH_2 symmetric (~2850 cm^{-1}), CD_2 antisymmetric (~2195 cm^{-1}), and CD_2 symmetric (~2090 cm^{-1}) vibration modes was determined using Spectra Calc software (Galactic Industries Corp., Salem, NH). Antisymmetric and symmetric vibration modes yielded similar results; we show CH_2 symmetric and CD_2 antisymmetric modes because the baseline was least disturbed by water absorbances in these spectral regions.

^{31}P nuclear magnetic resonance spectroscopy

MLVs at 10 mM total phospholipid were prepared as described, except that the hydrating buffer contained 20% (v/v) D_2O. After a minimum of 1 day of hydration, each sample was transferred to a 10-mm-diameter NMR tube (Wilmad Glass Co., Buena, NJ). Proton noise-decoupled free induction decays were collected at 10–50°C using a Varion 500 Unity Plus spectrometer operating at 202.3 MHz with the following instrument settings: sweep width, 50 kHz; pulse width, 20 μs; acquisition time, 0.55 s; receiver delay, 0.5 s; number of transients, $\geq$ 500. An exponential multiplication corresponding to line broadening of 50 Hz (fluid state) or 100–200 Hz (gel state) was applied to the accumulated free induction decays before Fourier transformation.

Protein kinase C purification

The Ca^{2+}-dependent isozyme PKC-α and the Ca^{2+}-independent isozyme PKC-η were purified from Sf-9 insect cells infected with recombinant baculovirus containing the specific isozyme construct by sequential chromatography on Q-Sepharose and phenyl-Superose (both from Pharmacia Biotechnology, Uppsala, Sweden). The baculovirus constructs were kindly

provided by Drs. P. Parker (Protein Phosphorylation Laboratory, Lincoln's Inn Fields, London, England) and D. Fabbro (Ciba-Geigy, Basel, Switzerland). Enzyme purity was confirmed by sodium dodecyl sulfate polyacrylamide gel electrophoresis followed by silver staining, and by Western blotting using isozyme-specific rabbit polyclonal antibodies (Santa Cruz Biotechnology, Santa Cruz, CA). PKC concentration was determined by a phorbol ester binding assay (Sando and Young, 1983). Purified enzyme was stored in 30% (w/v) glycerol and 20 mM MOPS, pH 7.5, at −80°C. Enzyme was thawed and diluted 1:7 or 1:4 (v/v) with MOPS/KCl buffer just before the kinase assays. The enzyme remained ~90% intact, as estimated by gel electrophoresis followed by silver staining, after incubation for 1 h at 35°C, the highest temperature of the kinase assays.

Assay of protein kinase C activity

Kinase activity was measured as the ability of PKC-α or PKC-η to phosphorylate lysine-rich histone III-S. The reaction mixture of 75 μl total volume contained 3–5 nM PKC, 2.7–4.0 mM total lipid, 10 μM histone, 40 μM ATP spiked with [γ-^{32}P]ATP to 1.6–3.7 Ci/mmol, 5 mM $MgCl_2$, 20 mM MOPS, 100 mM KCl, and 0.1 mM EGTA (pH 7.5). Assays with PKC-α also contained $CaCl_2$ buffered with EGTA to 5 μM free Ca^{2+}. Before aliquoting, the lipid was heated above the main transition and vortexed extensively. Lipid was equilibrated at the temperature of the assay, PKC was added, and the mixture was further incubated at the desired temperature. The reaction was initiated by adding a temperature-equilibrated substrate mixture: histone, [γ-^{32}P]ATP, ± Ca^{2+}, in MOPS/KCl buffer containing 5 mM $MgCl_2$. Linear reaction kinetics were maintained at all temperatures at which the assay was performed: the reaction was allowed to proceed for 40 min at 2°C or 45 s at 35°C for assays with PKC-α and 15 min at 13°C for assays with PKC-η. The reaction was terminated by spotting 60 μl of the reaction mixture onto Whatman P-81 cation exchanger paper (Whatman International, Maidstone, England). The papers were washed three times with 50 mM NaCl to remove unreacted ATP. The amount of ^{32}P transferred to histone was determined by measuring the Cerenkov radiation emitted from the dried papers.

RESULTS

Physical analysis of DMPC/DMPS/DO multilamellar vesicles

DSC

The excess heat capacity function for DMPS/DO MLVs as a function of χ_{DO} is shown in Fig. 1 *A*. When $\chi_{DO} \leq 0.17$, the main transition greatly broadens and shifts to lower temperatures with increasing χ_{DO}. However, between $\chi_{DO} = 0.17$ and $\chi_{DO} = 0.32$, a broad component and a narrow component coexist in the thermograms, consistent with compositional heterogeneity at temperatures below and within the main transition. Because the more cooperative transition grows at the expense of the broader one as χ_{DO} increases, the more cooperative transition is attributed to the melting of a phase enriched in DO. When $\chi_{DO} \geq 0.40$, the main transition remains essentially unchanged. The onset and termination temperatures of the main transition as a function of χ_{DO}, i.e., the apparent solidus and liquidus boundaries, were estimated from the heating scans and are shown in Fig. 1 *B*. The solidus boundary does not vary significantly when $\chi_{DO} \geq 0.17$, consistent with phase separation in the gel state at these compositions. In general, the compositions of two coexisting gel phases can be estimated from the compositions at which the invariance in the solidus

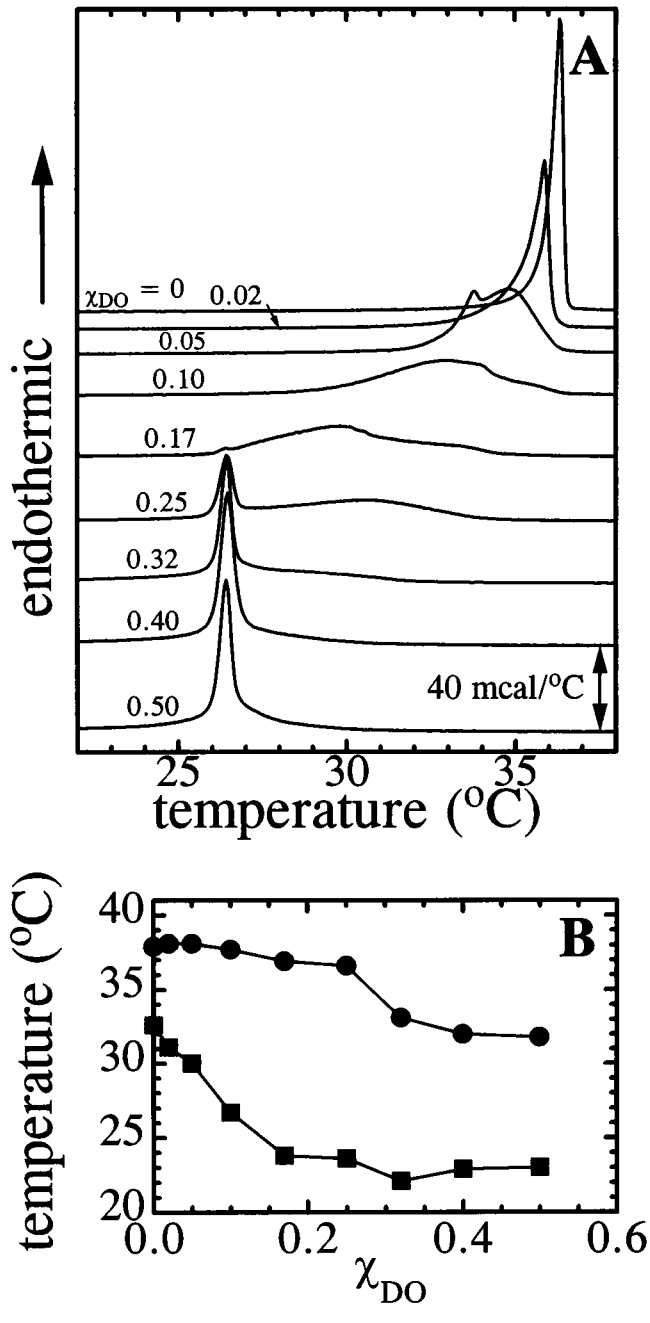

FIGURE 1 (*A*) Excess heat capacity functions for DMPS/DO MLVs at the values of χ_{DO} indicated within each panel. (*B*) Onset (■) and termination (●) temperatures of the gel-to-fluid phase transition as a function of χ_{DO}. Thermograms were up-scans from 0 to 60°C at 10°C/h. Each sample had 9.3 mM DMPS. The hydrating buffer was MOPS/KCl without divalent cations.

boundary begins and ends. Because it was not possible to estimate the DO-rich phase boundary in this way, we considered this phase boundary to be the highest value of χ_{DO} where the thermogram exhibits coexisting broad and narrow components. The data suggest that a DO-poor phase with $\chi_{DO} \approx 0.17$ and a DO-rich phase with $\chi_{DO} \approx 0.4$ coexist throughout this range of compositions in the gel state. Another striking feature of Fig. 1 *B* is that the liquidus

boundary does not appear to vary significantly when $\chi_{DO} \leq 0.25$. This result is consistent with a tendency for the DMPS and DO components to demix in the fluid state as well. It thus appears likely that DO-poor and DO-rich domains of fluctuating size and composition coexist at temperatures above the main transition.

DMPC/DO binary mixtures were analyzed by DSC in a similar way. The excess heat capacity function for DMPC/DO MLVs as a function of χ_{DO} is shown in Fig. 2 *A*. A pretransition was observed with pure DMPC at approximately 14°C. When $\chi_{DO} = 0.05$, a much smaller pretransition, with ~10% of the enthalpy change of the pretransition at $\chi_{DO} = 0$, was observed at approximately 8°C (not on-scale in Fig. 2 *A*). No pretransition was observed when $\chi_{DO} \geq 0.10$. The main transition is greatly broadened and shifted to lower temperatures upon incorporation of DO. However, this shift is not as pronounced as with DMPS/DO mixtures. Compositional heterogeneity at temperatures below and within the main transition is again suggested by the coexistence of broad and sharp components in the thermograms. With DMPC/DO mixtures, a sharp component is clearly evident by $\chi_{DO} = 0.10$, suggesting that DMPC and DO are less miscible than are DMPS and DO.

The estimates of solidus and liquidus boundaries of DMPC/DO MLVs (Fig. 2 *B*) are rather unusual in that the apparent solidus boundary exhibits a minimum and the apparent liquidus boundary exhibits a maximum as χ_{DO} is varied. The DO-induced severe broadening when $\chi_{DO} = 0.05–0.15$, coupled with a relatively small change in transition temperature, may indicate that DO has a tendency to reside at the interface between coexisting gel and fluid phases, and that DO has comparable solubility in these two phases. The unusual shapes of the apparent solidus and liquidus boundaries are probably the result of the coexistence in the gel state of compositionally distinct phases with transition temperatures near that of pure DMPC. A cooperative transition attributed to the melting of a DO-rich phase is first apparent at $\chi_{DO} = 0.10$ and is centered at approximately 21°C. It increases in intensity with increasing χ_{DO} until $\chi_{DO} = 0.20–0.25$, at which point a second cooperative transition, centered at approximately 20°C, takes its place and increases in intensity until $\chi_{DO} = 0.30$. These data suggest that a DO-rich phase with $\chi_{DO} \approx 0.25$ (DMPC/DO mole ratio ≈ 3:1) forms from $\chi_{DO} \approx 0.1$ to $\chi_{DO} \approx 0.25$, and that at higher DO contents a DO-rich phase with $\chi_{DO} \approx 0.3$ (DMPC/DO mole ratio ≈ 2:1) forms.

At those compositions where there is a cooperative transition centered at approximately 20°C (i.e., $\chi_{DO} = 0.25–0.40$), we also observed an anomalous transition in which the apparent excess heat capacity function exhibits a maximum and a minimum. The temperature at which this transition occurred varied linearly with χ_{DO}: 36.7°C at $\chi_{DO} = 0.25$, 31.2°C at $\chi_{DO} = 0.30$, and 21.7°C at $\chi_{DO} = 0.40$ (only the latter is on-scale in Fig. 2 *A*). It is not clear what this transition represents, but its unusual shape indicates that it is a nonequilibrium phenomenon. It is not a lamellar-to-H_{II} phase transition, according to our ^{31}P NMR results.

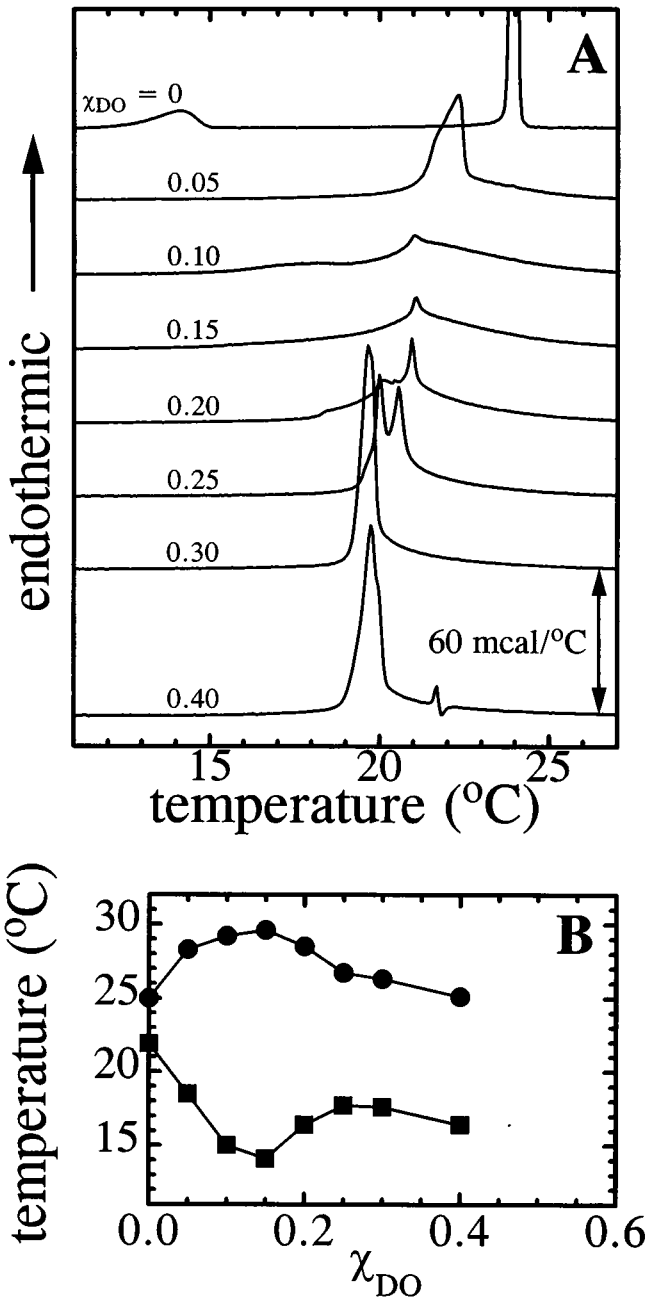

FIGURE 2 (*A*) Excess heat capacity functions for DMPC/DO MLVs at the values of χ_{DO} indicated within each panel. (*B*) Onset (■) and termination (●) temperatures of the gel-to-fluid phase transition as a function of χ_{DO}. Thermograms were up-scans from 0 to 60°C at 10°C/h. Each sample had 10 mM DMPC. The hydrating buffer was MOPS/KCl without divalent cations. The thermogram of pure DMPC is off-scale; the peak reaches a maximum of 400 mcal/degree above baseline and is 0.18°C wide at half height.

The excess heat capacity function for [DMPC/DMPS (1:1, mol/mol)]/DO MLVs as a function of χ_{DO}, as well as the estimates of solidus and liquidus boundaries, is shown in Fig. 3. The results are similar to those obtained with the

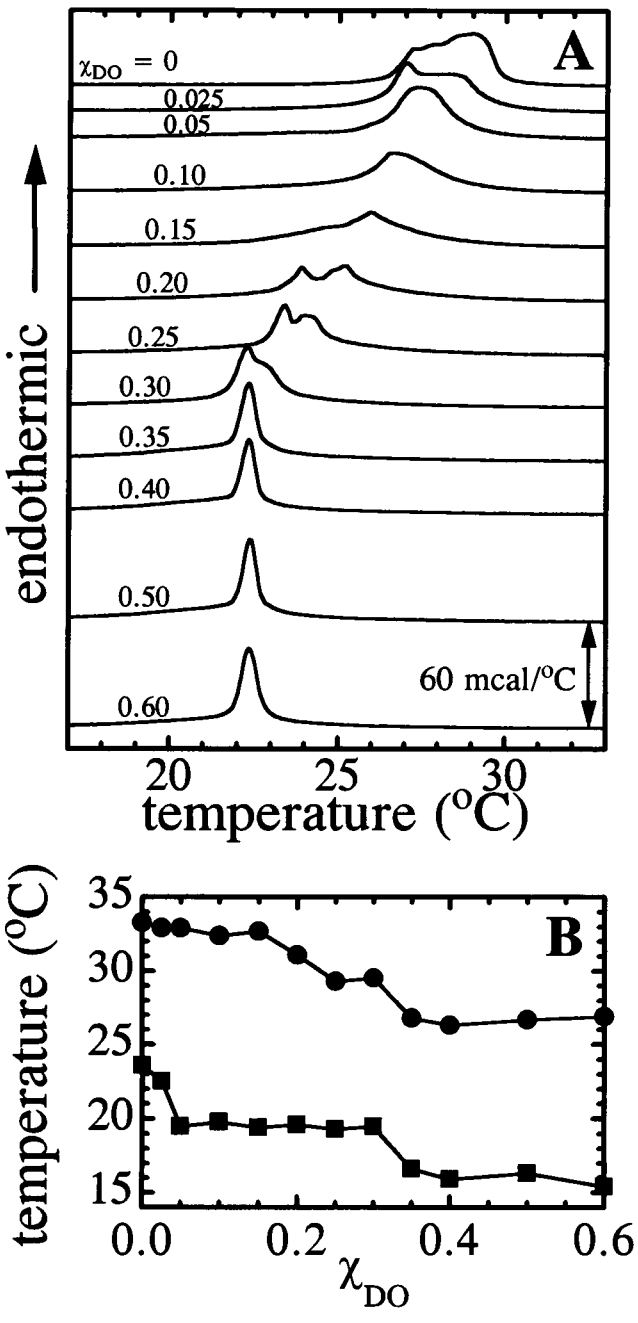

FIGURE 3 (*A*) Excess heat capacity functions for [DMPC/DMPS (1:1, mol/mol)]/DO MLVs at the values of χ_{DO} indicated within each panel. (*B*) Onset (■) and termination (●) temperatures of the gel-to-fluid phase transition as a function of χ_{DO}. Thermograms were up-scans from 0 to 60°C at 10°C/h. Each sample had 10 mM total phospholipid. The hydrating buffer was MOPS/KCl without divalent cations.

binary mixtures. The data strongly support gel/gel immiscibility from χ_{DO} = 0.05–0.10 to χ_{DO} = 0.30–0.35, as well as significant lateral heterogeneity at temperatures above the main transition.

A notable difference between the ternary mixtures and the binary mixtures is that with the former the transition attributed to the melting of a DO-rich phase gradually decreases in temperature and becomes more cooperative as χ_{DO} increases throughout the region of gel/gel immiscibility (Fig. 3 *A*). The lowest χ_{DO} at which this transition is apparent is χ_{DO} = 0.15, and this transition, centered at approximately 24°C, is quite broad relative to those observed with binary mixtures. The broadening could be caused by one of the two phospholipid components preferentially partitioning to the DO-rich domains, with this partitioning being more pronounced in the gel state than at temperatures within or above the main transition. This kind of preferential interaction of DO with one phospholipid component would be most pronounced at values of χ_{DO} just above that of the DO-poor phase boundary. Thus, the gradual increase in cooperativity of the peak attributed to the DO-rich phase as the relative amount of this phase increases (i.e., as χ_{DO} approaches the DO-rich phase boundary) is consistent with such a preferential interaction. Because the transition temperature of this peak *decreases* with increasing χ_{DO} throughout the compositions of gel/gel immiscibility, these data suggest that DO preferentially interacts with the higher melting phospholipid, i.e., DMPS, in DMPC/DMPS/DO ternary mixtures. The decrease in transition temperature is attributed to the DMPS/DMPC mole ratio within the DO-rich phase gradually decreasing toward 1 as the DO-rich phase boundary is approached. If DO had preferentially interacted with DMPC, we would have expected the transition temperature of the peak attributed to the DO-rich phase to *increase* with increasing χ_{DO}. This reasoning assumes that χ_{DO} in the DO-rich gel phase does not vary significantly as overall χ_{DO} is varied (i.e., that the system follows the Gibbs phase rule relatively well in the gel state).

With each of the three systems analyzed by DSC, the enthalpy change per mole of total phospholipid (i.e., DMPC + DMPS) associated with the gel-to-fluid phase transition (ΔH_{PL}) was found to be relatively independent of χ_{DO} (Fig. 4). When the enthalpy change is calculated in terms of total lipid (i.e., including DO), ΔH decreases linearly with increasing χ_{DO}, with a total loss in ΔH predicted (via extrapolation) by χ_{DO} = 0.9–1.0 (see the inset of Fig. 4). Either DO does not make a significant contribution to ΔH or there are compensating effects, with at least a portion of DO participating in the main transition while the contribution of phospholipid to ΔH is reduced.

Another striking feature of the DSC data is that when $\chi_{DO} > \sim 0.3$ with each of the systems, the main transition remains essentially unchanged as χ_{DO} is varied, not only with respect to ΔH_{PL}, but also with respect to peak shape and transition temperature (Figs. 1–3). These results are consistent with the coexistence of a lamellar phase having $\chi_{DO} \approx 0.3$ and a separate phase of a much higher DO content, when overall $\chi_{DO} > \sim 0.3$. The only system studied where there is thermotropic evidence for such a phospholipid-poor phase is DMPC/DO binary mixtures. With this system, a second cooperative transition was observed at approximately 6°C when $\chi_{DO} > \sim 0.4$, and this transition grew at the expense of the cooperative transition at ~20°C as χ_{DO} increased (data not shown). The α and β crystalline forms of pure DAG melt to an isotropic liquid on heating (Kodali et al., 1990); for DO, these transitions are

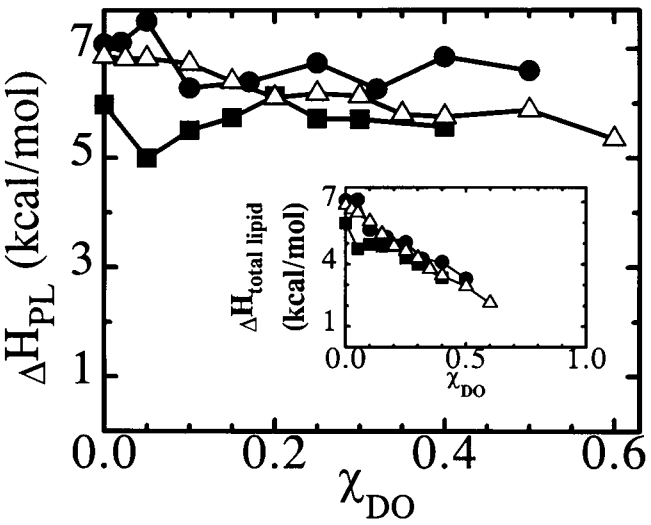

FIGURE 4 Enthalpy change per mole of total phospholipid (i.e., DMPC + DMPS), ΔH_{PL}, as a function of χ_{DO} in DMPS/DO (●), DMPC/DO (■), and [DMPC/DMPS (1:1, mol/mol)]/DO (△) MLVs. Measurements are from the thermograms of Figs. 1–3. (*Inset*) The same data plotted as enthalpy change per mole of total lipid (i.e., including DO) as a function of χ_{DO}.

near or below 0°C. It is possible that when $\chi_{DO} > \sim 0.3$ in the dispersions containing DMPS, essentially pure DO was excluded from the lamellar phase with $\chi_{DO} \approx 0.3$. Our ^{31}P NMR results (see below) confirm that the great majority of the DMPC and DMPS is present in lamellar structures, even at the highest DO contents analyzed ($\chi_{DO} = 0.60$). Although the location (i.e., in or out of the plane of the bilayer) of the phase extremely enriched in DO was not determined, its presence does not appear to significantly affect the activation of PKC (see below).

Corroborating evidence that a new phase forms when overall $\chi_{DO} > \sim 0.3$ is our finding that it was not possible to prepare large unilamellar vesicles (LUVs) at these compositions, regardless of the DMPC/DMPS mole ratio. At these very high DO contents, macroscopic strings (white, opaque, a few tenths of a millimeter in diameter) formed on both sides of the 0.1-μm-pore size polycarbonate filter. The formation of these macroscopic strings also occurred when we attempted to extrude pure DO.

FTIR spectroscopy

The main transition of DMPC/DMPS/DO MLVs was also monitored by FTIR spectroscopy to address several questions that arose during the DSC experiments: 1) Are DMPS/DO interactions more favorable than DMPC/DO interactions in ternary mixtures? 2) Is the relatively cooperative transition observed in the DSC thermograms when $\chi_{DO} > \sim 0.1$ due to a phase enriched in the DO component? and 3) To what extent does each lipid component participate in the main transition, i.e., why does ΔH_{PL} not vary significantly with χ_{DO}? An advantage of using FTIR to monitor the main transition is that it is possible to analyze the melting behavior of each component of ternary mixtures separately by making use of analogs of DMPC and DMPS with perdeuterated acyl chains (i.e., d_{54}-DMPC and d_{54}-DMPS). The temperature dependence of the conformational disorder (i.e., the *gauche/trans* ratio) of perdeuterated acyl chains and that of natural protonated acyl chains can be simultaneously analyzed within one sample by monitoring both CD_2 and CH_2 vibration modes, which are separated from one another by ~ 650 cm^{-1} because of the vibrational isotope effect (Mantsch and McElhaney, 1991).

In this way the melting behavior of d_{54}-DMPC and d_{54}-DMPS in ternary systems was compared by making use of [d_{54}-DMPC/DMPS (1:1, mol/mol)]/DO and [DMPC/d_{54}-DMPS (1:1, mol/mol)]/DO mixtures, respectively (Fig. 5). Note that perdeuteration of the acyl chains lowers the main transition by approximately 4°C for DMPC and by approximately 2°C for DMPS. When $\chi_{DO} = 0$, the main transition is already fairly broad (in agreement with our DSC results and the published DMPC/DMPS phase diagram; Silvius and Gagné, 1984), because there are equimolar amounts of PC and PS, phospholipid species that are known to have a tendency to demix in PC/PS binary mixtures, even in the fluid state (Huang et al., 1993; Hinderliter et al., 1994). The data of Fig. 5 *A* and Table 1 show that d_{54}-DMPC melts predominantly on the low-temperature side of this relatively broad transition, whereas d_{54}-DMPS melts on the high temperature side. This result, consistent with partial demixing of PC and PS components at temperatures below and within the main transition, is not an artifact caused by comparing two separate samples. A similar result is obtained when both of these samples are considered individually: the phospholipid that melts at a lower temperature when in pure form melted on the low-temperature side of the main transition in both cases (see Table 1).

The FTIR data also suggest partial demixing of the PC and PS components when $\chi_{DO} = 0.23$ (Fig. 5 *B*), a composition that according to the DSC data of Fig. 3 exhibits significant lateral heterogeneity of the lipid components at temperatures below and within the main transition. At this composition, the melting profiles of the natural protonated lipids are fairly similar (Table 1); this is consistent with the incorporation of a large fraction of DO and phospholipid into DO-rich domains when overall $\chi_{DO} = 0.23$. The presence of DO broadens the melting profiles and shifts them to lower temperatures, consistent with the DSC results. Because the putative DO-rich phase has a lower melting temperature and a more cooperative transition than does the putative DO-poor phase at this composition (see Fig. 3 *A*), we predicted that a strong tendency of DO to interact preferentially with the PS component would result in a more pronounced shift to lower temperatures and less broadening of the melting profile of d_{54}-DMPS, relative to that of d_{54}-DMPC. Although the data of Fig. 5 *B* uphold these predictions to some extent, the effects are subtle, suggesting that any preferential interaction of DO with DMPS is not overwhelmingly strong in this system.

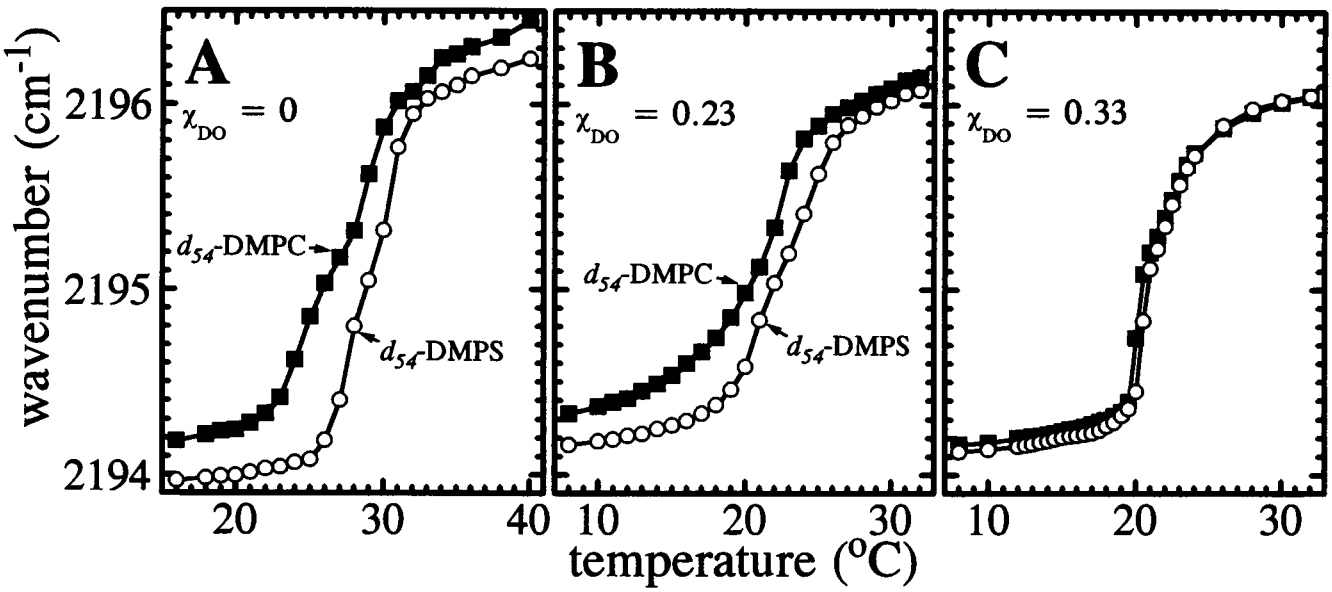

FIGURE 5 Melting of d_{54}-DMPC and d_{54}-DMPS in lipid mixtures as determined by the temperature dependence of the frequency of the CD_2 antisymmetric vibration mode of d_{54}-DMPC in [d_{54}-DMPC/DMPS (1:1, mol/mol)]/DO MLVs (■) and of d_{54}-DMPS in [DMPC/d_{54}-DMPS (1:1, mol/mol)]/DO MLVs (○) at (*A*) χ_{DO} = 0, (*B*) χ_{DO} = 0.23, and (*C*) χ_{DO} = 0.33. Each sample was hydrated at 15 mM total phospholipid with MOPS/KCl without divalent cations. Lipid was pelleted with a clinical centrifuge, and the concentrated sample (50–100 mM lipid) was analyzed. Data were collected by scanning up from 2 to 40–44°C. The time between successive spectra was ~15 min.

When DO content is raised to χ_{DO} = 0.33, a composition near that where the DSC thermograms reduce to a single sharp component (see Fig. 3 *A*), the phospholipid melting profiles are virtually superimposable (Fig. 5 *C*), with the transition temperature of each lipid component being virtually independent of the phospholipid deuterated (Table 1). The lipids no longer appear to be melting as separate components but rather as one entity. Because χ_{DO} = 0.33 is approximately the composition of the putative DO-rich phase, as estimated from the DSC data of Fig. 3, no preferential partitioning of one phospholipid component to this phase is expected. This three-component system has a remarkably cooperative gel-to-fluid phase transition, with very little apparent demixing of PC and PS. These data suggest that a new type of phase, enriched in the DO component (with a phospholipid/DO mole ratio near 2:1, i.e., in this case a DMPC/DMPS/DO mole ratio near 1:1:1), is formed in this system and that this DO-rich phase is fundamentally different from the DO-poor phase with regard to lipid mixing properties.

TABLE 1 Transition temperatures of the deuterated and of the natural protonated lipids in d_{54}-DMPC/DMPS/DO and DMPC/d_{54}-DMPS/DO MLVs as estimated by FTIR

χ_{DO}	Phospholipid content (PC/PS mole ratio = 1:1)	Transition temperature (°C) of the lipid(s) having acyl chains: Deuterated	Protonated
0	d_{54}-DMPC/DMPS	27.4	32.2
0	DMPC/d_{54}-DMPS	29.1	28.0
0.23	d_{54}-DMPC/DMPS	21.2	21.1
0.23	DMPC/d_{54}-DMPS	22.4	21.4
0.33	d_{54}-DMPC/DMPS	20.7	20.3
0.33	DMPC/d_{54}-DMPS	21.0	20.7

For each sample, the temperature dependences of the frequency of the CH_2 symmetric and of the CD_2 antisymmetric vibration modes were determined simultaneously (the latter is shown in Fig. 5). The change in wavenumber from the onset to the termination of the main transition was estimated, and the transition temperature is the temperature at which 50% of this change had taken place.

FTIR spectroscopy was also used to compare the melting profile of DO in d_{54}-DMPC/DO, [d_{54}-DMPC/d_{54}-DMPS (1:1, mol/mol)]/DO, and d_{54}-DMPS/DO MLVs (Fig. 6). As a control, it was verified that there was no detectable CH_2 symmetric vibration mode when χ_{DO} = 0 with these samples. The data of Fig. 6 confirm that at least a portion of the DO component is participating in the main transition (in each sample, the per-deuterated phospholipids melted over the same range of temperatures as did DO; data not shown). Thus, the essentially constant value of ΔH_{PL} (calculated per mole of phospholipid) as χ_{DO} is varied (Fig. 4) cannot be attributed to DO not melting. ΔH_{PL} may be virtually independent of χ_{DO} because of compensating effects, with the contribution of DO to ΔH_{PL} increasing and the contribution of the phospholipid components to ΔH_{PL} decreasing with increasing χ_{DO}. Consistent with such a phenomenon is the general observation that the magnitude of the change in wavenumber as d_{54}-DMPC and d_{54}-DMPS pass through the main transition decreases as χ_{DO} increases in binary and ternary mixtures (e.g., Fig. 5). These results are consistent with the phospholipid acyl chains becoming more disordered in the gel state and/or more ordered in the fluid state as χ_{DO} increases.

The data of Fig. 6 also show that the melting profiles of DO virtually overlay (except with respect to transition tem-

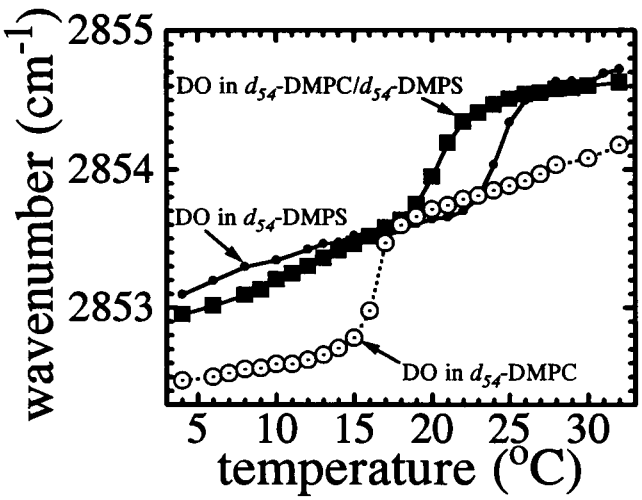

FIGURE 6 Melting of DO in lipid mixtures as determined by the temperature dependence of the frequency of the CH_2 symmetric vibration mode of DO in d_{54}-DMPS/DO (●), d_{54}-DMPC/DO (⊙), and [d_{54}-DMPC/d_{54}-DMPS (1:1, mol/mol)]/DO (■) MLVs at χ_{DO} = 0.25, 0.25, and 0.23, respectively. Sample preparation, range of temperatures, and time between successive spectra were as in Fig. 5.

perature) when the phospholipid composition is d_{54}-DMPC/d_{54}-DMPS (1:1, mol/mol) or pure d_{54}-DMPS. Apparently, the acyl chains of the DO component have a somewhat higher *gauche/trans* ratio in both the gel and fluid states in these mixtures relative to the d_{54}-DMPC/DO mixture. This phenomenon was observed at all values of χ_{DO} analyzed (χ_{DO} = 0.20–0.45) and is consistent with DO preferentially interacting with PS.

^{31}P NMR spectroscopy

To search for potential DO-induced isotropic motions of the phospholipids and/or H_{II} phase formation, ^{31}P NMR spectroscopy was employed. In NMR spectra, an isotropic resonance is often observed together with the broad anisotropic lineshape typical of MLVs tens of degrees below a lamellar-to-H_{II} phase transition (e.g., Gagné et al., 1985), implying that highly curved structures can form in bilayers that have some propensity to form the H_{II} phase, but under conditions in which no H_{II} phase is present. We analyzed DMPC/DO, [DMPC/DMPS (1:1, mol/mol)]/DO, and DMPS/DO MLVs from χ_{DO} = 0 to χ_{DO} = 0.6, and found ^{31}P NMR lineshapes typical of only lamellar structures at temperatures below, within, and above the main transition (the range tested was 10–50°C), in the absence and presence of 5 mM Mg^{2+}; no isotropic resonances were observed (data not shown). The only exception to this was at χ_{DO} = 0.6 with DMPC/DO binary mixtures, where evidence for a nonlamellar phase was evident at temperatures above the main transition. Otherwise, throughout the range of compositions and temperatures tested, DO does not appear to induce the phospholipids to form nonlamellar phases or regions of high bilayer curvature.

Protein kinase C activation using DMPC/DMPS/DO vesicles as the lipid activator

Equilibration of MLVs with Mg^{2+}

The ultimate goal of this work was to compare the membrane physical properties of DMPC/DMPS/DO vesicles with their ability to support PKC activity. Because Mg^{2+} was required for the PKC assays, we equilibrated [DMPC/DMPS (1:1, mol/mol)]/DO MLVs with 5 mM Mg^{2+}. In general, the presence of 5 mM Mg^{2+} shifted the main transitions approximately 5°C to higher temperatures and broadened the curves by approximately 6°C at half height (data not shown). The effect of Mg^{2+} on the thermotropic phase behavior of DMPS has been studied by Hauser (1991). At Mg^{2+} concentrations greater than 8 mM, a Mg^{2+}-DMPS complex is formed with a transition temperature of 98°C. This phase grows at the expense of the original phase as the Mg^{2+} concentration is increased further. We found that the presence of 5 mM Mg^{2+} did not significantly decrease ΔH_{PL} of the main transition of [DMPC/DMPS (1:1, mol/mol)]/DO MLVs (data not shown). Thus, at this concentration, the main effect of Mg^{2+} is to increase the ionic strength of the aqueous medium.

PKC activity

The ability of [DMPC/DMPS (1:1, mol/mol)]/DO MLVs to activate the Ca^{2+}-dependent isozyme PKC-α was evaluated at temperatures above (35°C) and below (2°C) the main transition (Fig. 7). A very low free Ca^{2+} concentration (5 μM) was included in these assays simply as a cofactor for PKC-α. The effect of this low Ca^{2+} concentration on lipid physical properties is expected to be negligible in the presence of 5 mM Mg^{2+} and 100 mM KCl. At 35°C, PKC activity was extremely low when $\chi_{DO} \leq 0.05$, but activity increased gradually with increasing χ_{DO} from $\chi_{DO} \approx 0.1$ to $\chi_{DO} \approx 0.4$ (Fig. 7 *A*). Thus, in the fluid state, PKC activity gradually increased with increasing χ_{DO} over the range of compositions where DSC suggests an increase in the amount of DO-rich domains (Fig. 3).

At 2°C, the activation of PKC-α by [DMPC/DMPS (1:1, mol/mol)]/DO MLVs clearly exhibited a maximum as χ_{DO} was varied (Fig. 7 *B*). There was very little activity when $\chi_{DO} \leq 0.05$, but there was a pronounced peak in PKC activity between $\chi_{DO} \approx 0.1$ and $\chi_{DO} \approx 0.3$. At higher DO contents, activity was essentially constant at 20–25% of the activity at the maximum. The range of compositions over which there was enhanced PKC activation corresponds to the range of compositions where there is gel/gel immiscibility, as estimated by DSC (Fig. 3). These data indicate that PKC is activated relatively inefficiently by the DO-rich gel phase by itself, but the coexistence of this phase with the DO-poor gel phase can dramatically enhance PKC activation.

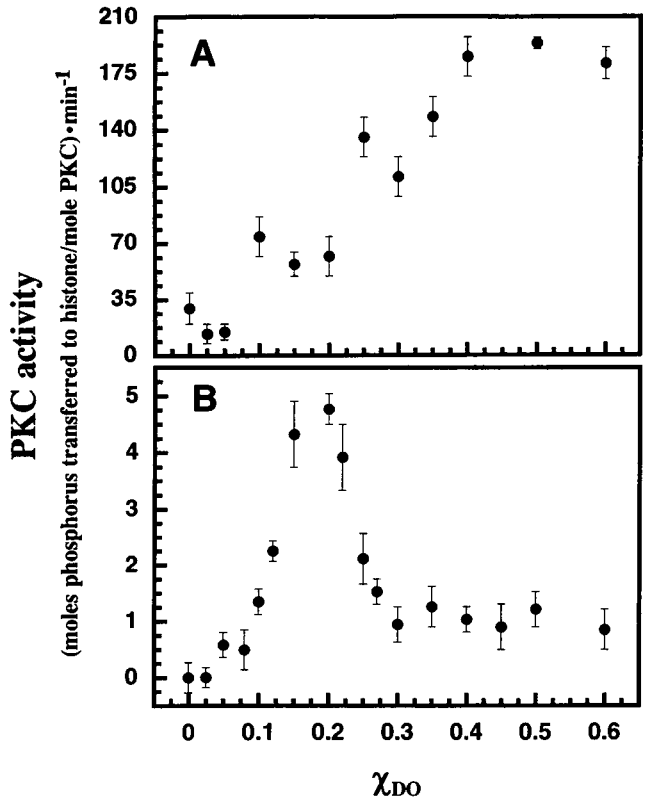

FIGURE 7 PKC-α activity as a function of χ_{DO} in [DMPC/DMPS (1:1, mol/mol)]/DO MLVs at (*A*) 35°C and (*B*) 2°C. Each sample contained 2.7 mM total lipid equilibrated with 5 mM Mg^{2+} in MOPS/KCl buffer. $CaCl_2$, buffered with EGTA to 5 μM free Ca^{2+}, was included in the reaction mixture to act as a cofactor for the enzyme. The amount of ^{32}P transferred to histone was measured for 45 s at 35°C and 40 min at 2°C; linear reaction kinetics were maintained at both temperatures. Each point represents the mean ± the range of duplicate (35°C) or the mean ± the standard deviation of triplicate (2°C) determinations. The lipid-free background (32,000 ± 2000 cpm at 35°C and 23,000 ± 3000 cpm at 2°C) was subtracted from each point and the errors were added. Maximum phospholipid-dependent activity corresponded to 157,000 ± 3000 cpm at 35°C (χ_{DO} = 0.50) and 106,000 ± 6000 cpm at 2°C (χ_{DO} = 0.20).

To evaluate the effects of both Ca^{2+} and multilamellar structure on these results, the activation of the Ca^{2+}-dependent isozyme PKC-α (with 5 μM free Ca^{2+}) and the Ca^{2+}-independent isozyme PKC-η (without Ca^{2+}) was compared using [DMPC/DMPS (1:1, mol/mol)]/DO 0.1 μm diameter LUVs in the gel state (13°C) as the lipid activator. The χ_{DO} dependence of normalized kinase activity was essentially identical for both isozymes, and it was quite similar to that found with gel-state MLVs, i.e., activity was significant only when $\chi_{DO} > 0.05$, and there was a pronounced maximum in activity at $\chi_{DO} = 0.15$ (data not shown). We preferred using MLVs in the PKC assays because the range of compositions over which LUVs could be prepared was limited to $\chi_{DO} = 0-0.3$, as discussed above. The similarity between MLVs and LUVs in the χ_{DO} dependence of PKC activation has been noted before (Bolen and Sando, 1992).

DISCUSSION

Physical properties of DMPC/DMPS/DO multilamellar vesicles

We have examined a three-component vesicle system, the ability of which to activate PKC is highly dependent on DO content. Our DSC results strongly suggest that DO-poor and DO-rich domains coexist in this lipid system from $\chi_{DO} \approx 0.1$ to $\chi_{DO} \approx 0.3$. The observations that support this conclusion include: 1) a broad and a sharp component were observed together in the DSC thermograms of MLVs from $\chi_{DO} \approx 0.1$ to $\chi_{DO} \approx 0.3$ (Figs. 1–3), consistent with compositional heterogeneity at temperatures below and within the main transition; 2) the onset temperature of the main transition as a function of χ_{DO} (i.e., the solidus boundary) was essentially invariant throughout this same range of compositions (Figs. 1–3), suggesting DO-poor/DO-rich phase separation at temperatures below the main transition; and 3) with the exception of the DMPC/DO binary mixture, the liquidus boundary was remarkably insensitive to χ_{DO} throughout this range of compositions (Figs. 1 and 3), implying that DO-poor and DO-rich domains also coexist at temperatures above the main transition.

Other phospholipid/DAG systems where the coexistence of DAG-poor and DAG-rich domains has been observed include DMPC/dimyristoylglycerol (DM) (Heimburg et al., 1992) and dipalmitoyl-PC/dipalmitoylglycerol (DP) (López-García et al., 1994b; Quinn et al., 1995). In both binary mixtures, gel/gel immiscibility exists from ~0 to ~0.45 mole fraction DAG, and the DAG-rich phase was examined by various biophysical techniques and regarded as a compound formation. These DAG-rich phases have remarkably cooperative gel-to-fluid phase transitions, as do the DO-rich phases we report here. One difference between our results and these others is that the compositional phase boundaries of gel/gel immiscibility are significantly closer to one another in our system (i.e., $\chi_{DO} \approx 0.1$ and $\chi_{DO} \approx 0.3$ compared to ~0 and ~0.45 mole fraction DAG). This difference may be due to the dissimilarity between the acyl chains of DO and those of DMPC and DMPS, with regard to length and degree of unsaturation. This acyl chain mismatch may cause DO to pack relatively poorly in the DO-rich gel phase, shifting both compositional phase boundaries.

Heimburg and co-workers (1992) used regular solution theory to analyze the DMPC/DM phase diagram in the region where DM is the minority component. The results are consistent with the coexistence of a DM-poor phase and a DM-rich compound, with a DMPC/DM mole ratio near 1:1, at temperatures above the main transition. The authors suggest that the 1:1 compound may be stabilized in the fluid state by intermolecular hydrogen bonding between the hydroxyl group of DM and the ester carbonyls of DMPC. Furthermore, the x-ray diffraction studies of Quinn and co-workers (1995) have provided direct evidence of immis-

cibility in the fluid state of dipalmitoyl-PC and the 1:1 complex of dipalmitoyl-PC and DP. Both of these results are important because they suggest that DAG-rich domains can be formed even when the lipid is in the fluid state, as it is in most physiological systems. Our DSC results are also consistent with DAG-poor/DAG-rich domain coexistence at temperatures above the main transition.

Taken together, our DSC and FTIR results suggest that the DO-rich phase in [DMPC/DMPS (1:1, mol/mol)]/DO vesicles has a mole ratio near 1:1:1 and is fundamentally different from the DO-poor phase with respect to lipid mixing properties. The strikingly cooperative main transition when $\chi_{DO} > \sim 0.3$ (Figs. 3 *A* and 5 *C*) and the virtually superimposable melting profiles of each lipid component when $\chi_{DO} = 0.33$ (Fig. 5 *C* and Table 1) are consistent with a relatively ordered array of lipid headgroups in the DO-rich domains. Intermolecular hydrogen bonding between DO and the phospholipids may stabilize such an array. DAG and PS both have a headgroup capable of acting as a hydrogen bond donor and acceptor. In contrast, the headgroup of PC can participate in intermolecular hydrogen bonds only as a hydrogen bond acceptor. Thus, DAG may participate more readily with PS than with PC in a hydrogen bond network, resulting in more favorable PS/DAG interactions relative to PC/DAG interactions.

Experimental evidence for such a preferential interaction is provided by our DSC results. With DMPS/DO mixtures, a cooperative transition attributed to the melting of a DO-rich phase is not apparent in the thermograms until $\chi_{DO} = 0.17$ (Fig. 1 *A*), whereas such a cooperative transition is clearly evident by $\chi_{DO} = 0.10$ with DMPC/DO mixtures (Fig. 2 *A*). This suggests that DMPC and DO are less miscible than are DMPS and DO. A comparison of the published phase diagrams of dipalmitoyl-PC/DP (López-García et al., 1994b) and dipalmitoyl-PS/DP (López-García et al., 1994a) binary mixtures leads to a similar conclusion, with the difference between PC/DAG and PS/DAG miscibility apparently being greater when the acyl chains are matched. With DMPC/DMPS/DO ternary mixtures, evidence for a preferential interaction of DO with DMPS is provided by the DSC thermograms of Fig. 3 *A*, which show a gradual increase in cooperativity and a concomitant decrease in transition temperature of the peak attributed to the DO-rich phase as the relative amount of this phase increases.

Any tendency for DO to interact preferentially with DMPS over DMPC would concentrate DMPS within DO-rich domains most significantly at compositions where only a small fraction of the total lipid is in these domains (i.e., at compositions just above the DO-poor phase boundary). The resultant concentrating of PS would increase the negative membrane surface potential in these regions, perhaps facilitating the binding of positively charged macromolecules, such as PKC and PKC substrates. The lipid binding studies of Orr and Newton (1992a) have shown that PS molecules tend to cluster around PKC. Furthermore, Yang and Glaser (1995) used fluorescence digital imaging microscopy to visualize the colocalization of myristoylated alanine-rich C kinase substrate (i.e., the MARCKS peptide) and PS in domains; the formation of these domains is apparently related to PKC activation. These kinds of colocalizations may be due to a thermodynamic coupling between the membrane binding of enzyme or substrate and a lipid structural change associated with a tendency for PS to cluster.

PS has a tendency to cluster in PC/PS binary mixtures, even in the fluid state (Huang et al., 1993; Hinderliter et al., 1994); this may be partially due to the potential for PS headgroups to hydrogen bond with one another. However, the net negative charge of the PS headgroup has an inhibitory effect on the clustering of PS. It is possible that DAG interacts with PS in such a way that the charge repulsion between PS headgroups is mitigated, allowing PS to become concentrated within localized regions more readily. Although the requirement for 1,2-*sn*-DAG (Rando and Young, 1984; Rando, 1988) and the L stereoisomer of PS (Lee and Bell, 1989; Newton and Keranen, 1994) for maximum PKC activity argues for specific DAG and PS binding sites on PKC, it is conceivable that these isomers are essential for a specific interaction in the lipid headgroup region, perhaps a particular hydrogen bonding configuration, which facilitates enzyme activation.

Protein kinase C activation by DMPC/DMPS/DO vesicles

The formation of DO-rich domains in [DMPC/DMPS (1:1, mol/mol)]/DO vesicles is apparently related to PKC activation. PKC was activated significantly only when $\chi_{DO} \geq 0.10$ (Fig. 7), i.e., at compositions where the DSC data are consistent with DO-rich domain formation (Fig. 3). When the temperature was above the main transition, PKC activity simply increased gradually as χ_{DO} was increased to the DO-rich phase boundary, i.e., $\chi_{DO} \approx 0.3$. In contrast, when the temperature was below the main transition, PKC activity clearly exhibited a maximum as χ_{DO} was varied over this range. These results suggest that the formation of DO-rich domains is related to PKC activation, and when the lipid is in the gel state, the *coexistence* of DO-poor and DO-rich phases also contributes to PKC activation.

There are several possible explanations for why PKC activity exhibited a maximum between the DO-poor and DO-rich phase boundaries when the lipid was in the gel state (Fig. 7 *B*):

1. If there is a tendency for lipids to laterally phase separate or to form distinguishable domains, and if PKC preferentially associates with one type of domain, PKC will cluster on the membrane surface. This clustering will enhance the probability of enzyme oligomerization. If PKC activation is related to the extent of oligomerization, maximum activity will be observed somewhere in the region of compositional or structural domain coexistence. For example, Heimburg and Biltonen (1996) have shown that proteins which bind preferentially either to the gel phase or to the fluid phase exhibit maximum clustering at a temperature

within the main transition. The quantitative details of this phenomenon depend on the temperature or composition at which domain formation begins to occur and on the partitioning of the protein between the coexisting domains.

2. If PKC activation is facilitated by the binding of enzyme to the interface between coexisting DO-poor and DO-rich phases, PKC activity would be expected to exhibit a maximum at a composition where the amount of interface between DO-poor and DO-rich phases is a maximum (i.e., near the percolation threshold).

3. Because the DMPC/DMPS mole ratio is held constant at 1:1, the overall mole fraction of DMPS decreases as overall χ_{DO} increases. If PKC is very sensitive to the DMPS/DO mole ratio within either the DO-poor or the DO-rich phase, PKC activity might be expected to depend on χ_{DO} in a complex manner. In the region of DO-poor/DO-rich phase coexistence, it is likely that the compositions of both phases change as overall χ_{DO} is varied, because DO may preferentially interact with DMPS and the system probably does not strictly follow the Gibbs phase rule. These three possible explanations for a maximum in PKC activity are not mutually exclusive.

PKC activity did not exhibit a pronounced maximum at an intermediate value of χ_{DO} when the lipid was in the fluid state (Fig. 7 *A*). This may be due to the DO-rich domains being smaller and/or shorter-lived in the fluid state. The strong dependence of PKC activity on whether the lipid was in the gel state or in the fluid state is consistent with an important role for changes in the size, lifetime, connectivity, and/or conformational disorder of DO-rich domains in modulating PKC activity.

Although maximum PKC activation in the gel state occurred at compositions where DO-poor and DO-rich phases coexist (compare Figs. 3 and 7 *B*), phase separation in general is not sufficient for PKC activation. For example, we found that gel/fluid phase coexistence in [DMPC/DMPS (1:1, mol/mol)]/DO LUVs at 24°C did not activate PKC when $\chi_{DO} < 0.1$ (unpublished observations). Moreover, Senisterra and Epand (1993) have shown that three different types of phase separations (gel/fluid, PC/PS, and phospholipid/cholesterol) do not enhance PKC activity. They did not have DAG in their systems, however. Our data suggest that DAG-induced phase separations can contribute to PKC activation. However, the formation of DAG-rich domains is clearly not sufficient for PKC activation; it is also important for an adequate amount of PS to be present. For example, Goldberg and co-workers (1994) found that DP-rich gel phase formation, in a system where the PC/PS mole ratio was 4:1, is not sufficient to activate PKC. Similarly, we found significantly lower PKC activity with DMPC/DMPS/DO vesicles when the DMPC/DMPS mole ratio was 3:1 or higher, even under conditions of DO-poor/DO-rich phase coexistence (unpublished observations). A similar dependence of PKC activity on the mole fraction of PS has been found with other PC/PS/DAG systems (Boni and Rando, 1985; Bazzi and Nelsestuen, 1987; Sando and Chertihin, 1996). Although DAG-rich domains tend to be formed at lower DAG contents in PC/DAG than in PS/DAG binary mixtures (e.g., compare Figs. 1 and 2), the presence of PS is essential for PKC activation. A requirement for domains containing both DAG and PS in the activation of PKC is consistent with the extensive literature identifying these lipids as the major activators of PKC in less well-characterized lipid systems (reviewed in Sando et al., 1992).

The physical properties of domains containing both DAG and PS that may contribute to PKC activation include an increased negative membrane surface potential, decreased hydration of the membrane surface, increased spacing between phospholipid headgroups, and an increased tendency to transiently expose regions of high bilayer curvature. The latter physical property was specifically addressed by our ^{31}P NMR experiments. According to our NMR results, the formation of DO-rich domains in the DMPC/DMPS/DO system does not correspond with the formation of highly curved structures. It cannot be ruled out that very small amounts of such structures form or that they are extremely enriched in DO, which is not detectable by ^{31}P NMR. Although we found no evidence for a relationship between PKC activity and isotropic phospholipid motions, it is possible that PKC activation would be more robust in a system where the DAG-rich domains have a greater tendency to be highly curved, such as when the phospholipid acyl chains are *cis*-unsaturated. For example, there is a correspondence between isotropic phospholipid motions in some unsaturated phospholipid/DAG systems and their ability to activate PKC (Goldberg et al., 1994) and numerous phospholipase A_2s (Dawson et al., 1984; Zidovetzki et al., 1992).

Collectively, our results corroborate the importance of both DAG and PS in activating PKC and suggest that the formation of compositionally distinct domains that contain both of these lipids contributes to activation of the enzyme. Our PKC activity measurements provide evidence not only that PKC is activated by the presence of these domains, but also that under certain conditions the *coexistence* of DAG-poor and DAG-rich regions further enhances PKC activity. This implies that the size, lifetime, connectivity, and/or conformational disorder of these domains affect the extent of PKC activation. The hypothesis that PKC activity is modulated by changes in these kinds of domain characteristics has important implications for both kinetic and equilibrium models describing PKC membrane binding and activation.

We thank Robert Doebler for assistance with the FTIR experiments, especially with regard to temperature control. We also thank Olga Chertihin, Prateek Gupta, Moira Resnick, and Betsy Vinton for their help during the purification of PKC isozymes and the subsequent kinase assays.

This work was supported by grants from the National Institutes of Health, U.S. Public Health Service (RO1 GM31184, RO1 GM37658, and PO1 GM47525). AD and AH were supported in part by National Institutes of Health Research Service Awards T32 DK07320 and T32 DK07642, respectively. A preliminary account of these findings was presented at the 39th Annual Meeting of the Biophysical Society, 1995, San Francisco, CA (Dibble et al., 1995). This manuscript is an extension of that work.

REFERENCES

Basu, A. 1993. The potential of protein kinase C as a target for anticancer treatment. *Pharmacol. Ther.* 59:257–280.

Bazzi, M. D., and G. L. Nelsestuen. 1987. Association of protein kinase C with phospholipid vesicles. *Biochemistry.* 26:115–122.

Bergelson, L. O., K. Gawrisch, J. A. Ferretti, and R. Blumenthal, editors. 1995. Special issue on domain organization in biological membranes. *Mol. Membr. Biol.* 12:1–162.

Bolen, E. J., and J. J. Sando. 1992. Effect of phospholipid unsaturation on protein kinase C activation. *Biochemistry.* 31:5945–5951.

Boni, L. T., and R. R. Rando. 1985. The nature of protein kinase C activation by physically defined phospholipid vesicles and diacylglycerols. *J. Biol. Chem.* 260:10819–10825.

Chiou, J.-S., P. R. Krishna, H. Kamaya, and I. Ueda. 1992. Alcohols dehydrate lipid membranes: an infrared study on hydrogen bonding. *Biochim. Biophys. Acta.* 1110:225–233.

Cunningham, B. A., T. Tsujita, and H. L. Brockman. 1989. Enzymatic and physical characterization of diacylglycerol-phosphatidylcholine interactions in bilayers and monolayers. *Biochemistry.* 28:32–40.

Das, S., and R. P. Rand. 1986. Modification by diacylglycerol of the structure and interaction of various phospholipid bilayer membranes. *Biochemistry.* 25:2882–2889.

Dawson, R. M. C., N. L. Hemington, and R. F. Irvine. 1983. Diacylglycerol potentiates phospholipase attack upon phospholipid bilayers: possible connection with cell stimulation. *Biochem. Biophys. Res. Commun.* 117:196–201.

Dawson, R. M. C., R. F. Irvine, J. Bray, and P. J. Quinn. 1984. Long-chain unsaturated diacylglycerols cause a perturbation in the structure of phospholipid bilayers rendering them susceptible to phospholipase attack. *Biochem. Biophys. Res. Commun.* 125:836–842.

De Boeck, H., and R. Zidovetzki. 1992. Interactions of saturated diacylglycerols with phosphatidylcholine bilayers: a ^{2}H NMR study. *Biochemistry.* 31:623–630.

Dibble, A. R. G., Y. A. Shen, J. J. Sando, and R. L. Biltonen. 1995. The role of lipid lateral heterogeneity in protein kinase C activation. *Biophys. J.* 68:A218.

Doebler, R., and P. W. Holloway. 1993. A small volume infrared transmission cell for aqueous solutions. *Anal. Biochem.* 212:562–564.

Edidin, M. 1992. The variety of cell surface membrane domains. *Comments Mol. Cell. Biophys.* 8:73–82.

Epand, R. M., and R. Bottega. 1988. Determination of the phase behavior of phosphatidylethanolamine admixed with other lipids and the effects of calcium chloride: implications for protein kinase C regulation. *Biochim. Biophys. Acta.* 944:144–154.

Exton, J. H. 1990. Signaling through phosphatidylcholine breakdown. *J. Biol. Chem.* 265:1–4.

Gagné, J., L. Stamatatos, T. Diacovo, S. W. Hui, P. L. Yeagle, and J. R. Silvius. 1985. Physical properties and surface interactions of bilayer membranes containing N-methylated phosphatidylethanolamines. *Biochemistry.* 24:4400–4408.

Goldberg, E. M., D. S. Lester, D. B. Borchardt, and R. Zidovetzki. 1994. Effects of diacylglycerols and Ca^{2+} on structure of phosphatidylcholine/phosphatidylserine bilayers. *Biophys. J.* 66:382–393.

Goldberg, E. M., D. S. Lester, D. B. Borchardt, and R. Zidovetzki. 1995. Effects of diacylglycerols on conformation of phosphatidylcholine headgroups in phosphatidylcholine/phosphatidylserine bilayers. *Biophys. J.* 69:965–973.

Hauser, H. 1991. Effect of inorganic cations on phase transitions. *Chem. Phys. Lipids.* 57:309–325.

Heimburg, T., and R. L. Biltonen. 1996. A Monte Carlo simulation study of protein-induced heat capacity changes and lipid-induced protein clustering. *Biophys. J.* 70:84–96.

Heimburg, T., U. Würz, and D. Marsh. 1992. Binary phase diagram of hydrated dimyristoylglycerol-dimyristoylphosphatidylcholine mixtures. *Biophys. J.* 63:1369–1378.

Hinderliter, A. K., J. Huang, and G. W. Feigenson. 1994. Detection of phase separation in fluid phosphatidylserine/phosphatidylcholine mixtures. *Biophys. J.* 67:1906–1911.

Huang, J., J. E. Swanson, A. R. G. Dibble, A. K. Hinderliter, and G. W. Feigenson. 1993. Nonideal mixing of phosphatidylserine and phosphatidylcholine in the fluid lamellar phase: computer simulation of experimental results shows clustering of each lipid type. *Biophys. J.* 64: 413–425.

Kikkawa, U., A. Kishimoto, and Y. Nishizuka. 1989. The protein kinase C family: heterogeneity and its implications. *Annu. Rev. Biochem.* 58: 31–44.

Kim, J., M. Mosior, L. A. Chung, H. Wu, and S. McLaughlin. 1991. Binding of peptides with basic residues to membranes containing acidic phospholipids. *Biophys. J.* 60:135–148.

Kingsley, P. B., and G. W. Feigenson. 1979. The synthesis of a perdeuterated phospholipid: 1,2-dimyristoyl-*sn*-glycero-3-phosphocholine-d_{72}. *Chem. Phys. Lipids.* 24:135–147.

Kodali, D. R., D. A. Fahey, and D. M. Small. 1990. Structure and polymorphism of saturated monoacid 1,2-diacyl-sn-glycerols. *Biochemistry.* 29:10771–10779.

Lee, M.-H., and R. M. Bell. 1989. Phospholipid functional groups involved in protein kinase C activation, phorbol ester binding, and binding to mixed micelles. *J. Biol. Chem.* 264:14797–14805.

López-García, F., V. Micol, J. Villalaín, and J. C. Gómez-Fernández. 1993. Infrared spectroscopic study of the interaction of diacylglycerol with phosphatidylserine in the presence of calcium. *Biochim. Biophys. Acta.* 1169:264–272.

López-García, F., J. Villalaín, and J. C. Gómez-Fernández. 1994a. Diacylglycerol, phosphatidylserine and Ca^{2+}: a phase behavior study. *Biochim. Biophys. Acta.* 1190:264–272.

López-García, F., J. Villalaín, J. C. Gómez-Fernández, and P. J. Quinn. 1994b. The phase behavior of mixed aqueous dispersions of dipalmitoyl derivatives of phosphatidylcholine and diacylglycerol. *Biophys. J.* 66: 1991–2004.

Mantsch, H. H., and R. N. McElhaney. 1991. Phospholipid phase transitions in model and biological membranes as studied by infrared spectroscopy. *Chem. Phys. Lipids.* 57:213–226.

Mosior, M., and S. McLaughlin. 1991. Peptides that mimic the pseudosubstrate region of protein kinase C bind to acidic lipids in membranes. *Biophys. J.* 60:149–159.

Nakamura, S.-I., and Y. Nishizuka. 1994. Lipid mediators and protein kinase C activation for the intracellular signaling network. *J. Biochem.* 115:1029–1034.

Newton, A. C., and L. M. Keranen. 1994. Phosphatidyl-L-serine is necessary for protein kinase C's high-affinity interaction with diacylglycerol-containing membranes. *Biochemistry.* 33:6651–6658.

Nishizuka, Y. 1986. Studies and perspectives of protein kinase C. *Science.* 233:305–312.

Orr, J. W., and A. C. Newton. 1992a. Interaction of protein kinase C with phosphatidylserine. 1. Cooperativity in lipid binding. *Biochemistry.* 31: 4661–4667.

Orr, J. W., and A. C. Newton. 1992b. Interaction of protein kinase C with phosphatidylserine. 2. Specificity and regulation. *Biochemistry.* 31: 4667–4673.

Ortiz, A., J. Villalaín, and J. C. Gómez-Fernández. 1988. Interaction of diacylglycerols with phosphatidylcholine vesicles as studied by differential scanning calorimetry and fluorescence probe depolarization. *Biochemistry.* 27:9030–9036.

Preiss, J., C. R. Loomis, W. R. Bishop, R. Stein, J. E. Niedel, and R. M. Bell. 1986. Quantitative measurement of *sn*-1,2-diacylglycerols present in platelets, hepatocytes, and *ras*- and *sis*-transformed normal rat kidney cells. *J. Biol. Chem.* 261:8597–8600.

Quinn, P. J., H. Takahashi, and I. Hatta. 1995. Characterization of complexes formed in fully hydrated dispersions of dipalmitoyl derivatives of phosphatidylcholine and diacylglycerol. *Biophys. J.* 68:1374–1382.

Rando, R. R. 1988. Regulation of protein kinase C activity by lipids. *FASEB J.* 2:2348–2355.

Rando, R. R., and N. Young. 1984. The sterospecific activation of protein kinase C. *Biochem. Biophys. Res. Commun.* 122:818–823.

Sando, J. J., and O. I. Chertihin. 1996. Activation of protein kinase C by lysophosphatidic acid: dependence on composition of phospholipid vesicles. *Biochem. J.* 317:583–588.

Sando, J. J., M. C. Maurer, E. J. Bolen, and C. M. Grisham. 1992. Role of cofactors in protein kinase C activation. *Cell. Signalling.* 4:595–609.

Sando, J. J., and M. C. Young. 1983. Identification of high-affinity phorbol ester receptor in cytosol of EL4 thymoma cells: requirement for calcium, magnesium, and phospholipids. *Proc. Natl. Acad. Sci. USA.* 80:2642–2646.

Senisterra, G., and R. M. Epand. 1993. Role of membrane defects in the regulation of the activity of protein kinase C. *Arch. Biochem. Biophys.* 300:378–383.

Sharkey, N. A., K. L. Leach, and P. M. Blumberg. 1984. Competitive inhibition by diacylglycerol of specific phorbol ester binding. *Proc. Natl. Acad. Sci. USA.* 81:607–610.

Silvius, J. R., and J. Gagné. 1984. Calcium-induced fusion and lateral phase separations in phosphatidylcholine-phosphatidylserine vesicles. Correlation by calorimetric and fusion measurements. *Biochemistry.* 23:3241–3247.

Slater, S. J., M. B. Kelly, F. J. Taddeo, C. Ho, E. Rubin, and C. D. Stubbs. 1994. The modulation of protein kinase C activity by membrane lipid bilayer structure. *J. Biol. Chem.* 269:4866–4871.

Stabel, S., and P. J. Parker. 1991. Protein kinase C. *Pharmacol. Ther.* 51:71–95.

Takai, Y., A. Kishimoto, Y. Iwasa, Y. Kawahara, T. Mori, and Y. Nishizuka. 1979. Calcium-dependent activation of a multifunctional protein kinase by membrane phospholipids. *J. Biol. Chem.* 254:3692–3695.

Tocanne, J. F. 1992. Detection of lipid domains in biological membranes. *Comments Mol. Cell. Biophys.* 8:53–72.

Walker, J. M., E. C. Homan, and J. J. Sando. 1990. Differential activation of protein kinase C isozymes by short chain phosphatidylserines and phosphatidylcholines. *J. Biol. Chem.* 265:8016–8021.

Walker, J. M., and J. J. Sando. 1988. Activation of protein kinase C by short chain phosphatidylcholines. *J. Biol. Chem.* 263:4537–4540.

Yang, L., and M. Glaser. 1995. Membrane domains containing phosphatidylserine and substrate can be important for the activation of protein kinase C. *Biochemistry.* 34:1500–1506.

Zhang, G., M. G. Kazanietz, P. M. Blumberg, and J. H. Hurley. 1995. Crystal structure of the cys2 activator-binding domain of protein kinase Cδ in complex with phorbol ester. *Cell.* 81:917–924.

Zidovetzki, R., L. Laptalo, and J. Crawford. 1992. Effect of diacylglycerols on the activity of cobra venom, bee venom, and pig pancreatic phospholipases A_2. *Biochemistry.* 31:7683–7691.